

SELECTIVE EMITTER IN N-TYPE C-SI SOLAR CELLS

J. Liu¹, G.J.M. Janssen¹, M. Koppes¹, E. J. Kossen¹, Y. Komatsu¹, J. Anker¹, A. Gutjahr¹,
 A. Vlooswijk², J. M. Luchies², O. Siareyeva³, E. Granneman³, I. Romijn¹
¹ECN, Solar Energy, P.O. Box 1, NL-1755 ZG Petten, The Netherlands
 The Netherlands, Phone: +31 224 564093; Fax: +31 224 568214; email: liu@ecn.nl
²Tempres Systems BV, Radeweg 31, 8171 MD Vaassen, The Netherlands
³Levitech BV, Versterkerstraat 10, NL-1322 AP Almere, The Netherlands

ABSTRACT: A selective emitter is expected to have a better blue response, less Auger recombination, less contact recombination and lower contact resistivity in industrially processed n-type solar cells. In this work, we present a controllable process to make a selective emitter by applying a printable resist on the emitter as a mask. In the subsequent etch process the p+ emitter can be selectively etched to optimize the passivation and conductivity. IV measurements from a batch of solar cells are presented to demonstrate the improvements on V_{oc} and I_{sc} . The mean efficiency of the SE cells is increased by 0.24% absolute compared to the standard homogeneous emitter cells resulting in a highest efficiency of 20.7%.

Keywords: n-type, selective emitter, selective etch

1 INTRODUCTION

For industrially processed n-type cells with printed contacts, one of the main factors limiting the efficiency is the recombination at the boron emitter contacts. Highly doped deep emitters are expected to provide a better shielding of the highly recombination metal contacts and enable low contact resistivity. However this type of homogeneous emitters shows losses due to the increased Auger recombination and free carrier absorption. The losses can be minimized with a selective emitter [1], as has been shown already by various authors for p-type solar cells [2,3,4] and n-type solar cells as well [5,6]. The selective emitter is formed by heavily doped emitter under the metal contacts and weakly doped emitter in the passivated areas. For p-type solar cells with n+ emitters, the selective emitter process has become redundant mainly because of improved n+ contacting pastes. However, for n-type solar cells this is still a challenge, and p+ contacts typically exhibit a very high recombination factor J_0 of about 3000 fA/cm² [7,8,9]. In this paper, we demonstrate that it is possible to achieve a selective emitter by a selective etch of the heavily doped p+ layer with a printable resist on the emitter as a mask, and that the expected gains are indeed observed.

2 NUMERICAL SIMULATION

To understand the relation between the recombination factor J_0 and the doping profile of the p+ emitter, we apply numerical modelling using the Atlas package from Silvaco as outlined in [8]. Our previous calculations illustrated the contact regions, especially from the emitter, are responsible for a major part of the recombination current [8].

Figure 1 shows the recombination factor on the front surface $J_{0\text{ front}}$ assuming the total J_0 is an area weighted average of the J_0 of the contacted area $J_{0\text{ con}}$ and of the passivated area $J_{0\text{ pass}}$. The blue curve in the figure represents the $J_{0\text{ front}}$ using $J_{0\text{ con}} = 3000$ fA/cm² and $J_{0\text{ pass}} = 80$ fA/cm², which corresponds to values valid for a typical 60 ohm/sq BBr₃ emitter. The red and green curves denote the $J_{0\text{ front}}$ obtained with emitters which have a reduced contact recombination factor. It shows that a reduction of the $J_{0\text{ con}}$ resulting from different emitter profiles will be more efficient than a reduction in $J_{0\text{ con}}$

from the reduced metal fraction. A reduction of 100 fA/cm² will result in a gain of approximately 10 mV in V_{oc} .

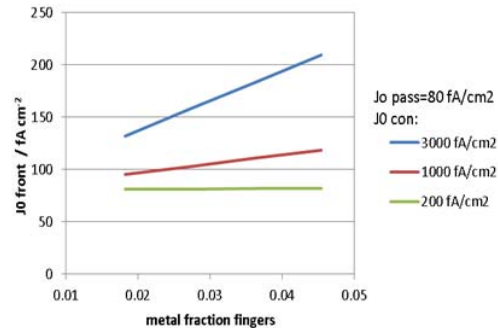


Figure 1: Calculated total J_0 value for the front surface as a function of the metal fraction with different contact passivation conditions

The recombination pre-factor $J_{0\text{ con}}$ can be calculated assuming thermal equilibrium at the contacts, i.e. an infinitely high value of the surface recombination velocity parameter. In order to obtain realistic values of the $J_{0\text{ con}}$, it must be assumed that there is an effective etch or penetration depth of the metal contacts into the emitter after firing the Al-Ag metallization paste [8]. We found that an effective etch depth about 250 nm can be assumed to explain the high $J_{0\text{ con}}$ as observed for the 60 ohm/sq BBr₃ emitter, as shown by the blue curve in Figure 2. Similar results were recently published by Edler et al [10]. For the 60 ohm/sq emitter $J_{0\text{ con}}$ increases sharply with increasing the penetration depth, due to increasingly less effective shielding of the contact. The green line shows the $J_{0\text{ con}}$ of the emitter calculated with a Gaussian profile corresponding to an R_{sheet} of 30 ohm/sq and a doping depth of about 800 nm. It indicates that a 30 ohm/sq emitter would be sufficient to reduce the contact recombination below 1000 fA/cm² for a metal penetration depth of 250 nm. It also shows that the shielding capacity of a heavy, deep emitter is less dependent on this etch depth. This allows a deep enough firing of the metallization into the emitter to obtain a low contact resistance and high FF, while still limiting the $J_{0\text{ con}}$ to 1000 fA/cm² and thus keeping a high V_{oc} .

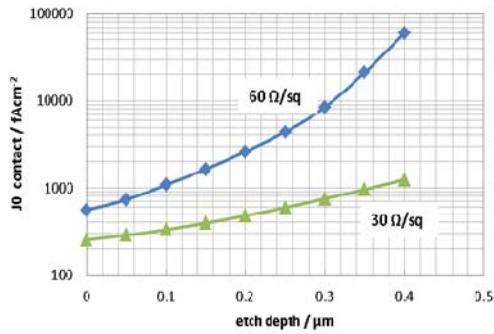


Figure 2: Calculated J_0 value on emitter contact as a function of the assumed penetration or etch depth of the metal contact

3 EXPERIMENTAL

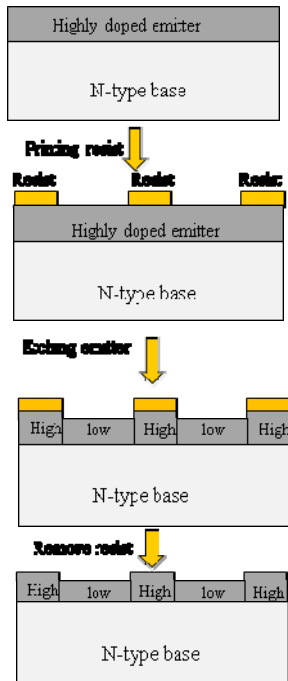


Figure 3: Process steps of the selective emitters

Textured n-type CZ wafers were used to make the SE solar cells. Figure 3 shows the process steps of formation of the selective emitters. A commercial resist is printed selectively on the p+ emitter after a Boron diffusion. Then a solution is used to etch selectively the p+ emitter. Since the achieved sheet resistance in the etched areas is dependent on the etching time and the etching conditions, the selective emitter can be obtained in a controllable manner.

4 RESULTS & DISCUSSION

4.1 Emitter profiles

Several diffusion profiles were generated by varying the diffusion temperature and diffusion time to achieve different R_{sheet} and different depth. We aimed to find a best suitable emitter profile as a start for the selective

emitter. Figure 4 displays four diffusion profiles measured by ECV. The reference emitter is 60 ohm/sq with a 0.5 μm depth, as shown in profile 1. Profile 2, 3 and 4 correspond to 3 different diffusion processes carried out at different temperatures. The temperatures from profile 2 to profile 4 is $T_2 < T_3 < T_4$. Sheet resistances for profile 2, 3 and 4 are 40 ohm/sq, 35 ohm/sq and 30 ohm/sq respectively.

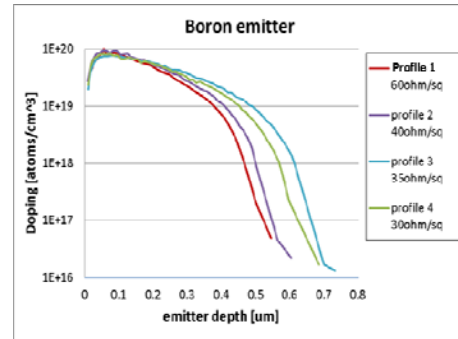


Figure 4: Doping profiles measured by ECV of different BBr3 diffused emitters

4.2 Effect on metal recombination

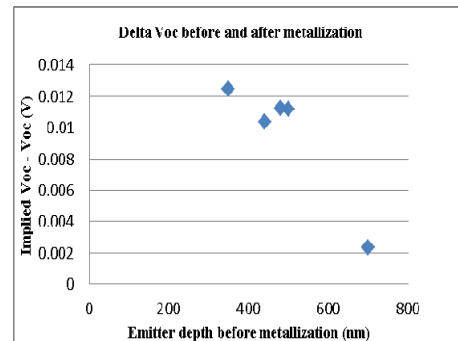


Figure 5: Differency between Implied Voc and Voc as a function of the emitter depth

As we know the $J_{0, con}$ values cannot be measured directly, but can be estimated by comparison of implied V_{oc} (iV_{oc}) value on non-metallized samples and V_{oc} value on finalized cells [11]. Figure 5 shows the difference between iV_{oc} and V_{oc} as a function of the emitter depth (using slightly different profiles from Figure 4). The drop in V_{oc} is reduced from 12 mV for shallow emitter (0.3 μm) to 2 mV for a deep emitter (0.7 μm). This indicates the deep emitter plays a critical role in minimizing the V_{oc} loss by more effective shielding of the minority charge carriers from reaching the metal contacts.

4.3 Passivated emitters

To obtain acceptable J_0 values for the passivated area of the emitter, the emitter is controllably etched and passivated by Al_2O_3 deposited with an industrial, spatial ALD system. Figure 6a shows the histogram of R_{sheet} after etching of different depth. Figure 6b shows the $J_{0, pass}$ of different diffusion profiles versus R_{sheet} between 40 ohm/sq to 90 ohm/sq. The J_0 value is extracted from the lifetime measurement by QSSPC on symmetrical p+/n/p+ emitter structures. This enables the selection of the optimal etch depth on the basis of the R_{sheet} - J_0 combination. By etching the emitter between the fingers, the R_{sheet} is increased but initially the J_0 is reduced due to reduction of the Auger recombination. At higher R_{sheet} the $J_{0, pass}$ saturates due to an

increasing contribution of surface recombination. However, it should be noticed the reference emitter, that had SiN_x passivation, actually has a lower J_0 than the etched emitters with the same sheet resistance. In the present range of emitters, the field passivation of Al_2O_3 layer is suppressed due to the high boron concentration on the surface [7][12]. The lowest J_0 is achieved by etching profile 3 by 250 nm and is around 55 fA/cm^2 for a 75 ohm/sq emitter, which is about 10 fA/cm^2 lower than for the 60 ohm/sq emitter. This shows the selective emitters made of the deep heavy diffusion profile can be tuned in the contact region to a better shielding effect and in the non-contact region to a better passivation effect.

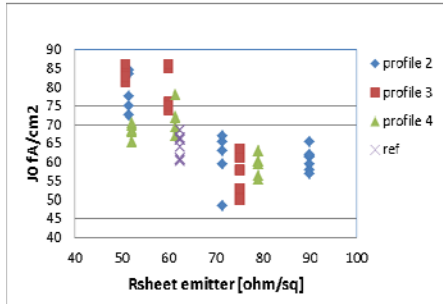
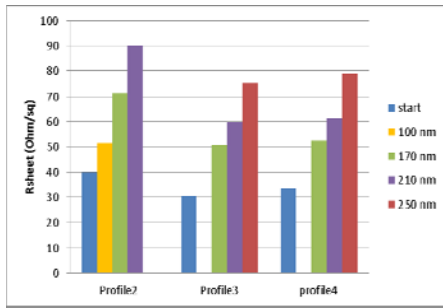


Figure 6a&6b: R_{sheet} (left) & J_0 (right) with respect to the etching depth on different doping profiles

4.4 Solar cells with selective emitter structures

The IV data of SE cells processed by profile 4 compared to the reference homogeneous emitter cells is shown in Table I. All the cells were fabricated on the 6 inch $180 \mu\text{m}$ thick n-type Cz-Si wafers. Reference cells were processed with a homogeneous emitter for comparison. The selective emitters were passivated with ALD $\text{Al}_2\text{O}_3/\text{SiN}_x$ stack layers.

Table I: IV data of reference cells with homogeneous emitter and SE cells (averaged over 5-7 cells) on profile 4

	Emitter (Ω/sq)	I_{sc} (A)	V_{oc} (V)	FF (-)	Eta (%)
Ref Ave	60	9.33	0.652	0.784	19.97
Ref Best		9.34	0.652	0.786	20.03
SE Ave	32/75	9.34	0.655	0.778	19.91
SE Best		9.37	0.657	0.776	19.99

The short circuit current is slightly better, which can be attributed to the better blue response of the high ohmic emitter between the fingers of the SE cells. Also the open circuit voltage of the SE cells is higher than that of the reference cells, which can be explained by less contact and Auger recombination. However, the fill factor of the SE cells is significantly lower than that of the reference cells, which results in a efficiency of SE cells lower than

the efficiency of reference cells. It can be noticed that the gain in V_{oc} is not as much as expected for SE cells. The reason can be that the BSF profile is not optimized yet for these cells, which can increase the relative importance of $J_{0\text{rear}}$, and become the limiting factor for the gain on V_{oc} .

To improve the performance of the SE cells, we optimized the metal pattern on the emitter side to reduce the series resistance loss in FF. In the latest experiment, we used the diffusion profile 3 for lowest J_0 , and no Al_2O_3 layers were made for passivation. Table 2 illustrates the IV data of reference cells with homogeneous emitter and SE cells on profile 3.

Table II: IV data of reference cells with homogeneous emitter and SE cells (averaged over 10 cells) on profile 3

	Emitter (Ω/sq)	I_{sc} (A)	V_{oc} (V)	FF (-)	Eta (%)
Ref Ave	60	9.29	0.66	0.788	20.25
Ref Best		9.33	0.66	0.79	20.37
SE Ave	35/75	9.29	0.663	0.795	20.49
SE Best		9.28	0.663	0.804	20.67

In this experiment, the V_{oc} for reference cell is 8mV higher than the previous experiment by applying an improved chemical cleaning process, which is beneficial for both front and rear side of the cell. Again the gain in the short circuit current and open circuit voltage is limited due to the non-optimized BSF. Even though the rise in open circuit voltage is still limited to 3 mV , it can be attributed to the less contact and Auger recombination in the emitter region. Similar to the Table I, the gain in V_{oc} from using a SE is probably limited by the BSF diffusion profile and BSF passivation. Compared to the first experiment, the FF is improved by applying new metal pattern, which more than compensates the series resistance loss in the SE cells.

The mean efficiency of the SE cells is increased by 0.24% absolute resulting in a highest efficiency of 20.7% . More optimizations can be done on the BSF diffusion profile and BSF passivation to achieve an even higher efficiency of the SE cells.

5 CONCLUSION

Within this study, we present the improvements of n-Pasha cell efficiency by making a selective emitter. The selective emitter has a deeper p+ profile under the contacts but a higher sheet resistance between the fingers. By optimization of the metallization pattern the fill factor could even be slightly improved compared to the reference case. Together with a gain in open circuit voltage this lead to a gain of 0.24% absolute in cell efficiency, and highest cell efficiency so far of 20.7% . The potential gain of the SE is even higher since the BSF quality and recombination becomes more limiting with improved emitters. Further re-optimization of the BSF is expected to result in both I_{sc} and V_{oc} increase.

6 ACKNOWLEDGEMENTS

The author would like to acknowledge the project partners in the project "NChanted" and "Orion".

7 REFERENCES

- [1] S.R. Wenham and M.A. Green “Laser grooved solar cell”, in US Patent, USA, 4,626,613, (1986)
- [2] T.C.Roder et al. “Add-on laser tailored selective emitter solar cells”, *Prog. Photovolt: Res. Appl.* 2010; 18:505-510
- [3] T. Lauermann et al. “INSECT: An inline selective emitter concept with high efficiencies at competitive process costs improved with inkjet masking technology”, 24th EUPVSEC, 2009, Hamburg, Germany
- [4] J. Kohler et al. “Laser doped selective emitters yield 0.5% efficiency gain”, 24th EUPVSEC, 2009, Hamburg, Germany
- [5] Y. Schiele et al. “Etch-back of p+ structures for selective boron emitters in n-type c-Si solar cells”, 4th SiliconPV, 2014
- [6] A. Edler et al. “Bifacial n-type solar cell with selective boron emitter”, 28th EUPVSEC, 2013, Paris, France
- [7] G.J.M. Janssen et al. “Front side improvements for n-Pasha solar cells”. 29th EUPVSEC, 2014, Amsterdam, The Netherlands
- [8] G.J.M. Janssen et al. “Power loss analysis of n-Pasha cells validated by 2D simulations”. 28th EUPVSEC, 2013, Paris, France
- [9] I.G. Romijn et al. “Industrial cost effective n-Pasha solar cells with >20% efficiency”. 28th EUPVSEC, 2013, Paris, France
- [10] A. Edler et al., “Metallization induced recombination losses of bifacial silicon solar cells”, *Progress in Photovoltaics* DOI: 10.1002/pip.2479, 2014
- [11] T. Fellmeth et al. *Energy Procedia* 8 115-121, 2011
- [12] L.E. Black, et al. *J.Appl.Phys.* 115, 093707, 2014